Pergamon

Int. J. Heat Mass Transfer. Vol. 40, No. 7, pp. 1585–1589, 1997

0017-9310/97 $17.00+0.00

PII: S0017-9310(96)00222-0

Compressible gas in porous media: a finite amplitude analysis of natural convection

P. H. STAUFFER†
Earth Science Board, UCSC, Santa Cruz, CA 95064, U.S.A.

and

L. H. AUER and N. D. ROSENBERG
Los Alamos National Laboratory, Los Alamos, New Mexico, U.S.A.

(*Received* 7 *November* 1995 *and in final form* 3 *June* 1996)

Abstract—The theory of thermally driven convection of dry air in a porous medium is reviewed. The critical Rayleigh number for air is the same as for liquid, $4\pi^2$, but the thermal gradient used is decreased by the adiabatic gradient of air. Because of the differences in the physical properties of air and water, initiation of convection requires the product of gradient and permeability to be thousands of times greater for air than for water. Finite amplitude analysis of the problem for $Ra < 300$ shows that: (1) the code predicts the onset of convection in an air filled porous medium; (2) at low thermal gradient, Ra vs Nu curves are nearly the same for air and water; (3) the slope of the Ra vs Nu curve matches well with experimental data reported by others for water; (4) time to steady state decreases approximately as the square root of Nusselt number. Copyright © 1996 Elsevier Science Ltd.

INTRODUCTION

The onset of convection in incompressible liquid in a porous medium has been considered many times, and a comprehensive treatment of this subject can be found in Nield and Bejan [1]. Much less work has been done, however, on the problem of ideal gas convection in porous media. Strauss and Schubert [2] include the compressibility term in their linear stability analysis (LSA), but restrict their analysis to steam saturated water (i.e. no free vapor phase). Saatdjain [3] neglects the pressure/volume contribution to the energy equation in his treatment of ideal gas porous convection. Nield [4] corrects Saatdjain and provides many insights into the differences between air and water, but provides only a brief LSA. Zhang [5] presents a complete LSA for moist gas convection in porous media that reduces to the solution of Nield when moisture content is zero. The reader is referred to this work for further details.

Nield [4] and Zhang [5] both show that the onset of convection in an ideal gas can be characterized by a critical Rayleigh number (Ra). The exact form of the definition of the Rayleigh numbers, however, is altered because of the effects of compressibility. To first order, the only difference is that for an incompressible fluid, like water, we have the Rayleigh number

$$Ra_{\text{liquid}} = \frac{\alpha H^2 \boldsymbol{g} c_p \Gamma \rho^2}{\mu \kappa}. \tag{1a}$$

whereas for air, we have a slightly different definition of the Rayleigh number:

$$Ra_{\text{air}} = \frac{H^2 K \boldsymbol{g}(c_p \Gamma - \boldsymbol{g})\rho^2}{T \mu \kappa}. \tag{1b}$$

The two definitions of the Rayleigh numbers are almost identical. For an ideal gas, $\alpha = 1/T$. The c_p term in Ra_{liquid} is replaced by $(c_p\Gamma - \boldsymbol{g})$ in the Ra_{air} definition. This result is analogous to Jeffrey's [6] conclusion that the Ra for compressible fluid convection (no porous medium) must be modified to account for the adiabatic gradient [4]. The change in the effective temperature gradient arises from the pressure dependence of the heat content of a fluid parcel. In an incompressible fluid, the internal energy depends only on the temperature. In a compressible gas, if a packet moves into a lower pressure region, it expands and cools, adiabatically reducing the effective temperature gradient. This means for air, Γ must be larger than an adiabatic gradient, $\boldsymbol{g}/c_p \approx 10^{-2}$ K m^{-1}, before the Rayleigh number even has a positive value. Below the adiabatic gradient, air convection is not possible for any values of system height (H) or permeability (K). Thus if we use Ra_{liquid}, but substitute an effective temperature gradient

$$\Gamma_{\text{eff}} = \Gamma - \frac{\boldsymbol{g}}{c_p}$$

† Also at the Los Alamos National Laboratory.

NOMENCLATURE

c_p	heat capacity of fluid at constant pressure
g	gravitational constant
H	thickness of system
K	permeability
Nu	Nusselt number
P	pressure of fluid
Q	heat content
Ra	Rayleigh number
T	temperature of gas and matrix (Kelvin)
ΔT	change in temperature across system
t	time
U	internal energy
$\mathbf{v}$	Darcy fluid flux
W	work
$\mathbf{z}$	downward unit vector.

Greek symbols

α	fluid thermal expansivity
Γ	$\Delta T/H$, temperature gradient
ϕ	porosity
κ	equivalent thermal conductivity
μ	viscosity of fluid
ρ	fluid density.

Subscripts

c	critical
eff	effective
m	matrix
s	steady state.

Superscript

$'$	total derivative with respect to time.

for Γ and $1/T$ for α, the two Rayleigh numbers are identical [4].

It is the values of the physical quantities appearing on the two Rayleigh number definitions that dominate the difference between the convective stability of subsurface water and air. Simple algebra shows that for a given geothermal gradient the critical permeability for onset of convection in a typical porous medium is three orders of magnitude greater for dry air than liquid water (Table 1).

The dramatic increase in the permeability needed to initiate convection in air is explained by the factors noted previously. While the lower viscosity and higher thermal expansion coefficient favor convection in air, these are more than off-set by the ρ^2 factor present in equations (1a) and (1b). Convection occurs when it is more efficient to move energy by the physical exchange of matter than by conduction of heat. While it is easy to convect large volumes of air, those volumes of air carry little energy, and that heat is rapidly dissipated by the conduction through the matrix, damping the convective motion.

The purpose of this paper is to examine convective flow in a porous medium filled with dry air heated from below. We present the theory, report finite amplitude results for Rayleigh numbers Ra up to 300, discuss the relationship between time to steady-state, Nusselt number (Nu) and Ra for these systems, and compare the results to those for similar systems saturated with liquid.

Table 1. Physical Properties of Air and Water at 293 K and 373 K†

Air		*Water*		
293 K	373 K	293 K	373 K	
ρ 1.205	0.946	998.2	958.4	kg m^{-3}
α 3×10^{-4}	2.7×10^{-3}	2.1×10^{-4}	7.1×10^{-4}	K^{-1}
κ 2.5×10^{-2}	3.2×10^{-2}	0.6	0.68	W m^{-1} K^{-1}
c_p 1006	1011	4182	4216	J kg^{-1} K^{-1}
μ 1.81×10^{-5}	2.18×10^{-5}	1.0×10^{-3}	2.83×10^{-4}	Pa s

† Values from appendices C and D, Bejan [11].

The motivation for this work comes from our study of the effects of volcanic intrusions into partially saturated rock. We seek to understand the spatial and temporal scale over which an intrusive event can have a significant effect on the transport of gases, both from the intrusion itself (e.g. SO_2) or at some distance from the intrusion. Firstly, we review the governing equations and verify the ability of the numerical code we use for our finite amplitude calculations to reproduce the critical Rayleigh number.

GOVERNING EQUATIONS

The basic equations which govern low velocity (Darcy flow regime) convective flow in porous media are well developed in the literature (e.g. Nield and Bejan [1], Strauss and Schubert [2], and Nield [4]). In the following form, rewritten from refs. [1, 2, 4] for clarity, the equations apply to single phase compressible as well as Bousinesq approximate incompressible fluids.

$$\phi\frac{\partial\rho}{\partial t}+\nabla\cdot\rho\mathbf{v}=0 \tag{2a}$$

$$\mathbf{v}=-\frac{K}{\mu}(\nabla P-\rho\mathbf{g}\mathbf{z}) \tag{2b}$$

$$(\rho c_p)_m\frac{\partial T}{\partial t}+(\rho Q')_f=\kappa\nabla^2 T \tag{2c}$$

where the matrix density, ρ_m, includes a correction for porosity. Equation (1c) can be reformatted in the

more traditional form of Nield [4]. By substitution of $Q' = U' - W'$, and bearing in mind the total derivative of a quantity (Q) includes an advective transport contribution as:

$$Q' = \frac{\partial Q}{\partial t} + \mathbf{v} \cdot \nabla \mathrm{Q}. \tag{2d}$$

We arrive, after some algebraic manipulation and thermodynamic substitutions, at:

$$(\rho c_p)_m \frac{\partial T}{\partial t} + (\rho c_p)_f T' - \alpha T P' = \kappa_{eff} \nabla^2 T. \tag{2e}$$

The difference between the convection of an incompressible liquid and the convection of a compressible gas arises from three basic causes. The first is the significantly smaller amount of energy contained in a given volume of gas compared to the same volume of liquid. The advective heat transport term, $\rho Q'$, of equation (2c) is directly proportional to the density, ρ. For example, even though the rate of change per unit mass, Q', is roughly the same for both water and gas, the fact that the density of air is three orders of magnitude lower makes convection in air much less efficient. The second cause is the much smaller buoyancy force ($\rho \boldsymbol{g}$, equation (2b)) for air, again due to the very large difference in the densities. For air,

$$\delta \rho \boldsymbol{g} = \rho \boldsymbol{g} \left(\frac{\delta P}{P} - \frac{\delta T}{T} \right) \tag{3a}$$

where the first term on the right hand side corresponds to the isothermal compressibility, β. For the incompressible case, only the thermal expansion term is retained as:

$$\delta \rho \boldsymbol{g} = \rho \boldsymbol{g} \alpha \delta T. \tag{3b}$$

The third is that the energy content of a given volume of air is pressure dependent whereas the energy content of a given volume of liquid is not. For air,

$$\rho Q' = c_p \rho T' - P'. \tag{4a}$$

In contrast, for a Boussinesq liquid,

$$\rho Q' = c_p \rho T'. \tag{4b}$$

Secondary factors that lead to real gases being more stable than an ideal gas include variations in α, c_p and μ with temperature [4]. Comparison between air and water material properties and their derivatives with temperature can be located in Nield and Bejan [1] and also Bejan [7].

FINITE AMPLITUDE ANALYSIS

In order to consider finite amplitude convection in air, one must go beyond the assumptions used in the linear stability analysis. This is especially important with air, since the strong temperature dependence of the thermodynamic properties of air leads to large differences in the Rayleigh number calculated at the hot versus cold ends of the convective cell. Note that in this paper, we will report all Ra values calculated at the mean temperature of the system after Davidson [8].

For the numerical analysis of the convection problem we have used the finite element heat and mass transfer code FEHM [9a, b]. Originally developed for use in geothermal reservoir modeling, FEHM is capable of simulating multi-phase transport of air, water, water vapor, and dilute solutes in fractures and porous media. FEHM solves these equations for the highly nonlinear equations for air convection using the Galerkin technique to discretize the spatial derivative, and a standard first order approach to the time discretization. Lobbato integration is used to evaluate integrals in the finite element equations and a modified Newton Raphson iterative procedure is used to solve the resulting system of equations. Dependence of material properties on pressure and temperature is represented as a cubic polynomial. The polynomial fits are based on National Bureau of Standards steam tables [10].

In our calculations, we assume that (1) flow is not affected by quadratic drag or boundary phenomenon (i.e. the creeping Darcy regime); (2) thermal equilibrium exists between the air and rock. The violation of either of these would require extra terms to modify the treatment of heat transfer. We address (1) first. The transition from creeping Darcy flow to inertial flow is determined by the value of the porous Reynolds number, Re_p. If $Re_p \ll 1$, all inertial and boundary effects are negligible. Even under the liberal assumption that our pore diameter is as large as 10^{-3} m, Re_p approaches unity only if the air velocity is above 0.015 m s^{-1}. Maximum air velocities reached during this study were 2×10^{-4} m s^{-1} at $Ra = 300$. With respect to issue (2), thermal equilibrium is reached if a temperature perturbation in the convective cell moves slowly compared to the time required to exchange energy over pore-scale lengths. Computations of energy transfer rates for FEHM (9a) show that thermal equilibrium is valid for water velocities below 10^{-5} m s^{-1}. Scaling the water results to air by the product of relative heat capacity, thermal conductivity, and density (Table 1), we come to the conclusion that a typical porous medium should be in approximate thermal equilibrium at air velocities below 1.7×10^{-3} m s^{-1}.

A simple two dimensional regular grid representing a 200 m square, broken into 49×49 rectangular elements, has been used for the simulations. The top and bottom boundaries have fixed temperatures while the side boundaries permit no flow with respect to either mass or energy (Fig. 1). Note that this choice of no flow lateral boundaries restricts the horizontal motion, and limits the possible planforms. For all the simulations presented here we use an initial mid-domain temperature of 60°C. The top and bottom boundaries are set to $60°C \pm 1/2\Delta T$. For each case, a non-flow calculation was used to generate the initial

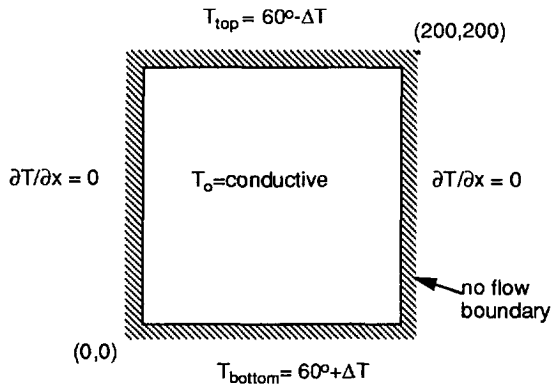

Fig. 1. Domain, boundary and initial conditions for finite amplitude numerical simulations reported in this study.

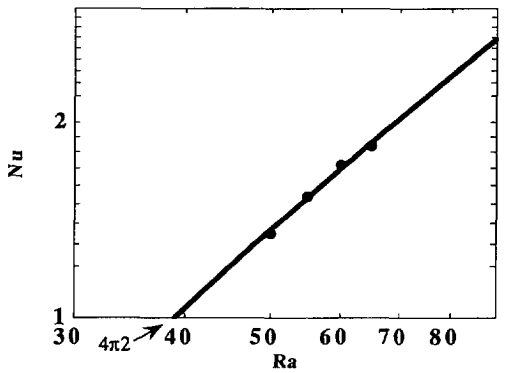

Fig. 3. *Nu* vs *Ra* for air from low *Ra* FEHM simulations.

temperature-pressure distributions as input for the stability test. Convection was set in motion by finite temperature perturbations (0.1–1°C) at selected bottom nodes.

Our major measure of the dynamics of convection in these systems is the computed Nusselt number, *Nu*, which is the ratio of the total flux to the purely conductive flux implied by the temperature gradient. We calculate *Nu* at the top and the bottom of the system numerically after the system has reached steady state. The criterion for determining a steady state is that a small rate of change in the temperature has been achieved. As one can see in Fig. 2, this time is well-determined. Error in the calculation of *Nu* is estimated to be between 2 and 3%.

FEHM RESULTS

We begin by validating FEHM's ability to predict the onset of convection in air. As we show below, FEHM reproduces the critical Rayleigh number remarkably well (Fig. 3). We determined Ra_c by a straight line fit through the results for four calculations at low Rayleigh extrapolated to $Nu = 1$. Nonlinear effects decrease with temperature gradient, so we used a low thermal gradient of 20°C km^{-1} for this analysis. By definition at Ra_c the time to set up convection is infinitely long so we must extrapolate the finite amplitude results to estimate the threshold value. The Ra_c determined from these FEHM results is 39, remarkably close to the linear stability prediction of $4\pi^2$.

Figure 4 shows all of our finite amplitude results for air and for water on a *Ra* vs *Nu* plot. As this figure shows, the results for air and water are nearly identical. See Table 1 for property values used in these simulations. The thermal gradient for these simulations was 20°C km^{-1} for air and 300°C km^{-1} for water. These results are in good agreement with a scaling analysis reported by Nield and Bejan [1] for systems saturated with water and experimental data reported by Kaneko *et al.* [11], Buretta and Berman [12] and Elder [13].

The relationship between *Nu* and time to steady state (t_s) is shown in Fig. 5. As this figure shows, the time to establish the convective flow is on the order to 1000 years for the system simulated here, and decreases as the strength of the convection increases. t_s scales in a simple way, decreasing in approximately direct proportion to the square root of *Nu*. This is true for a variety of thermal gradients and different system heights, scaled in Fig. 5 such that the product, $(KH\Gamma)$, remains constant. Scaling to determine times needed to reach steady state has proved useful in our current work. Another point of interest is that as

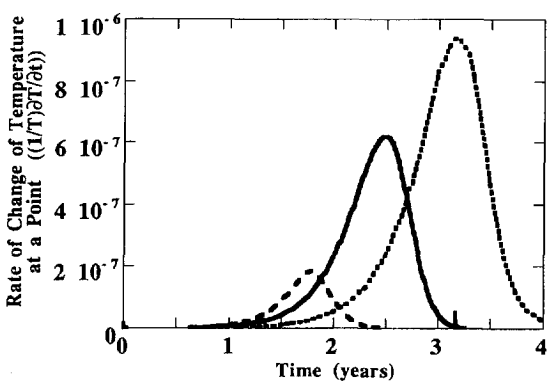

Fig. 2. Rate of change of temperature at a point vs time. We defined steady-state as approximately the 95th percentile of these curves.

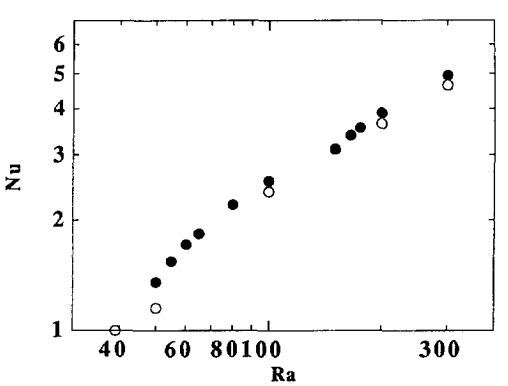

Fig. 4. *Nu* vs *Ra* for air and water from FEHM simulations. Filled circles represent results for air convection. Open circles represent results for water convection.

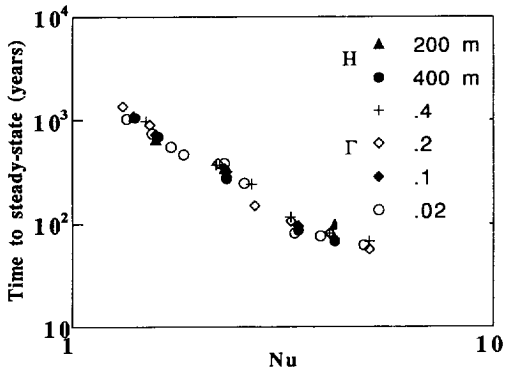

Fig. 5. Time to steady-state vs *Nu* for air from FEHM simulations for systems with several different thermal gradients and different heights.

Nusselt number approaches one from above, time to steady state quickly exceeds the time for a conductive profile to equilibrate, in agreement with observations reported by Elder [13].

We use *Nu* rather than *Ra* to bypass the problems of Ra_{air} varying so greatly in value from the top to the bottom of the system. Instead of using a mean value for the system temperature and plotting *Ra* vs t_s after Davidson [8], we have chosen to examine time to steady state as a function of the Nusselt number. The solution of the LSA equations for stability of integer wavelength cells predicts that multiple planforms are stable for a given *Ra*, each with a unique *Nu* [1]. Final planform pattern depends solely on initial conditions, thus a plot of *Ra* vs t_s would have several time points for a given *Ra*. The Nusselt number provides a single value for energy transport across a system at steady state and is therefore a more consistent parameter to plot vs time to steady state.

CONCLUSIONS

The equations governing convection of air in a porous medium are very similar to those of water. The compressibility of the air, however, does affect the apparent temperature gradient. Because the air cools adiabatically when it rises, the effective temperature gradient is correspondingly reduced. By including this term it is possible to define a Rayleigh number appropriate for the prediction of the onset of convection in air. The resulting critical Rayleigh number for air is the same as for water, $4\pi^2$, when the gradient in incompressible Rayleigh number is lowered by the adiabatic gradient of the gas. Even though the critical numbers are identical, it is much more difficult to induce convection in air than in water. In fact, the product of gradient and permeability must be thousands of times larger because of the very much lower density of the gas, which makes convection in air much less efficient in transporting energy than in water.

Finite amplitude analysis of the problem using the FEHM computer code show that (1) the numerical code predicts the onset of convection in air very well; (2) the *Ra* vs *Nu* curves for air (at low thermal gradients) and water are nearly identical; (3) the slope of this *Ra* vs *Nu* curve matches well with theory and experimental data reported by others for water; (4) time to steady state decreases approximately as the square root of *Nu*.

Acknowledgements—This work is part of magmatic hazards assessment studies being carried out under the management and funding of the U.S. Department of Energy's Yucca Mountain Site Characterization Project as part of the Civilian Radioactive Waste Management Program. Computational work described herein was done in a prototyping mode and was not subjected to full software quality assurance measures.

REFERENCES

1. Nield, D. A. and Bejan, A., *Convection in Porous Media*. Springer, Berlin, 1992.
2. Strauss, J. M. and Schubert, G., Thermal convection of water in a porous medium: effects of temperature and pressure dependent thermodynamic and transport properties. *Journal of Geophysical Research*, 1977, **82**, 325–333.
3. Saatdjain, E., Natural convection in a porous layer saturated with a compressible ideal gas. *International Journal of Heat and Mass Transfer*, 1980, **23**, 1681 1693.
4. Nield, D. A., Onset of convection in a porous layer saturated by an ideal gas. *International Journal of Heat and Mass Transfer*, 1982, **25**, 1605–1606.
5. Zhang, Y., Lu, N. and Ross, B., Convective instability of moist gas in a porous medium. *International Journal of Heat and Mass Transfer*, 1994, **37**, 129–138.
6. Jeffrey, H., The instability of a compressible fluid heated from below. *Proceedings of the Cambridge Philosophical Society*, 1930, **26**, 170–172.
7. Bejan, A., *Heat Transfer*. Wiley, New York. 1993.
8. Davidson, M. R., Natural convection of gas/vapor mixtures heated from below. *International Journal of Heat and Mass Transfer*, 1986, **9**, 1371–1386.
9. (a) Zyvoloski, G. A., Robsinon, B. A., Dash, Z. V. and Trease, L. L. Models and methods summary for the FEHMN application. Los Alamos national Laboratory document LA-UR-94-3787 Rev. 1, 1995. (b) Zyvoloski, G. A., Robinson, B. A., Dash, Z. V. and Trease, L. L., Users manual for the FEHMN application. Los Alamos National Laboratory document LA-UR-94-3788 Rev. 1, 1995.
10. Haar, L., Gallagher, J. S. and Kell, G. S., *NBS/NRC Steam, Tables*. Hemisphere, New York, 1984.
11. Kaneko, T., Mohtadi, M. F. and Aziz, K., An experimental study of natural convection in inclined porous media. *International Journal of Heat and Mass Transfer*, 1974, **17**, 129–138.
12. Buretta, F. J. and Berman A. S., Convective heat transfer in a liquid saturated porous layer. *Journal of Applied Mechanics*, 1976, **98**, 249–253.
13. Elder, J. W., Steady free convection in a porous medium heated from below. *Journal of Fluid Mechanics* 1967, **27**, 29–48.